DESIGN AND SIMULATION OF A C-BAND PYRAMIDAL HORN ANTENNA FOR WATER-LEVEL RADAR SENSORS

Ke-Ru Chou
Department of Electrical Engineering, National Taiwan Ocean University, Keelung, Taiwan, R.O.C.

Tzong-Dar Wu
Department of Electrical Engineering, National Taiwan Ocean University, Keelung, Taiwan, R.O.C.

Han-Nien Lin
Department of Communications Engineering, IC-EMC Research and Development Center, Feng-Chia University, Taichung, Taiwan, R.O.C.

Tai-Shan Liao
Instrument Technology Research Center, National Applied Research Laboratories, Hsinchu, Taiwan, R.O.C.

Kwong-Kau Tiong
Department of Electrical Engineering, National Taiwan Ocean University, Keelung, Taiwan, R.O.C. Department of Communications, Navigation and Control Engineering, National Taiwan Ocean University, Keelung, Taiwan, R.O.C., b0114@ntou.edu.tw

DESIGN AND SIMULATION OF A C-BAND PYRAMIDAL HORN ANTENNA FOR WATER-LEVEL RADAR SENSORS

Acknowledgements

DESIGN AND SIMULATION OF A C-BAND PYRAMIDAL HORN ANTENNA FOR WATER-LEVEL RADAR SENSORS

Ke-Ru Chou[1], Tzong-Dar Wu[1], Han-Nien Lin[2], Tai-Shan Liao[3], and
Kwong-Kau Tiong[1, 4]

ABSTRACT

A prototype C-band pyramidal horn antenna was fabricated after using High Frequency Structure Simulator (HFSS) software to simulate, analyze, and optimize the design parameters. The pyramidal horn antenna was designed to operate as a key detection component for disaster prevention and warning instruments in the domestic development of water-level radar sensor (WLRS). Experimental measurements showed the horn operating with a bandwidth of ~ 800 MHz from 5.4 GHz to 6.2 GHz with the central frequency at 5.8 GHz. The voltage standing wave ratio (VSWR) in the operating frequency range and the radiation pattern gains were measured to be smaller than 1.2 and larger than 16 dB, respectively. The experimental measurements compared well with the simulated results and met the design requirements.

I. INTRODUCTION

Two-thirds of Taiwan is comprised of subtropical mountainous regions. The monsoon season begins in May, which is characterized by rainstorms. During the summer and fall, typhoons assault Taiwan. When a typhoon leaves the region, it often introduces a southwesterly airstream. During typhoon season, rainfalls of more than 1000 mm in 2-3 days are not uncommon. Furthermore, the duration and spatial distribution of the rainfall is extremely non-uniform. The relatively steep slopes of the mountains in Taiwan and the excessive logging of forests have also adversely affected soil and water conservation. In addition, rivers in Taiwan are short and steep; and therefore, when the monsoon or typhoon brings rainstorms, heavy rainfall accumulates in the high ground will cascade down the steep mountain streams with such ferocity that can cause severe flooding and landslides. The formidable water or debris flow can scour bridges, breaking support columns of the bridges, washing away the bridge deck and houses in the downstream flatlands. These events can cause staggering loss of life and property. In order to alleviate the impact of the cataclysmic events, an early warning system must be developed. Monitoring water-level and flow velocity of rivers can provide crucial early warnings during the monsoon and typhoon seasons, and reliable readings can reduce flood damage and enhance the effectiveness of disaster warnings. The hydrological instruments used to monitor water-levels and velocities of the rivers can be categorized as contact or noncontact. Contact instruments are vulnerable to damage by violent flooding, whereas noncontact hydrological instruments do not share the same risk. However, among noncontact photoelectric instruments, only radar-based hydrological instruments can be used at night or during strong winds or rainstorms. Nevertheless, the radar-based instruments used in Taiwan are imported and expensive, and more importantly, their designs are based on the environmental parameters of their countries of origin. As a result, imported instruments are often not entirely suitable for local implementation. The differences in environmental parameters between Taiwan and other countries should require distinct design considerations. Therefore, designing hydrological instruments suitable for Taiwan is a critical focus of the plan to develop reliable technology for disaster warning systems.

Two basic and frequently used hydrological detection instruments are the WLRS and the flow-velocity radar sensor. Of these, the WLRS requires more complex installation and circuit solver technology, but it forms the core for all disaster-prevention radar instruments. Therefore, when developing

Fig. 1. Block diagram of the proposed WLRS prototype.

Fig. 2. Model of a pyramidal horn antenna.

new technology for the local hydrological instruments, the WLRS must be first established and tested.

A WLRS prototype has been designed and is now under construction for monitoring the water level of rivers. Fig. 1 shows the schematic block diagram of the proposed prototype WLRS. The prototype WLRS comprises the following components: a voltage control oscillator (VCO), which serves as the excitation source; a pyramidal horn for transmitting and receiving the reflected signals; a mixer for the comparison of the reflected signal with that of the transmitted signal to achieve low frequency signal, which will be amplified by a low noise amplifier and analyzed by a low frequency processing unit for the estimation of water level.

The test setup of the WLRS is designed to have less than 15 m footprint for antenna at a height of 30 m. Therefore, the limitation of the beam width of the horn antenna used for the proposed WLRS should be 28°. On top of that, as an indispensable component of a WLRS, the need of an enhanced gain for the antenna in limited space is also critical (Jasik and Johnson, 2000).

Horn antennas were first developed for military and scientific purposes and have been used since the early 19th century. However, widespread uses did not occur until World War II. Typical horn antennas exhibit either rectangular or conical structures. Rectangular structures can be subdivided into H-plane, E-plane, and pyramidal horn structures (Balanis, 2005; Elliott, 2003). Water-level sensor antennas typically use the pyramidal horn antenna design, for which a schematic model is shown in Fig. 2, with the inner dimensions of the aperture and WR187 rectangular guide feed to be $A \times B = 140$ mm $\times$ 100 mm and $a \times b = 47.55$ mm $\times$ 22.15 mm, respectively. The wall thickness is 2.5 mm. Pyramidal horn antenna is a type of aperture antenna, exhibiting the following characteristics: (1) the horns are constructed of aluminum for robustness, corrosion resistance, and high power sustainability; (2) the antenna structure should be simple and easy to design and manufacture; i.e. easy to be mechanically cut, chiseled, and welded (3) wide operating frequency range, low reflection losses, and high gains making it suitable for use as a communication antenna; (4) after the aperture of the antenna is determined, the antenna pattern and beam width will be fixed
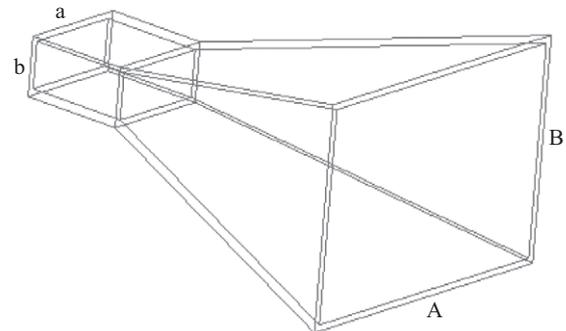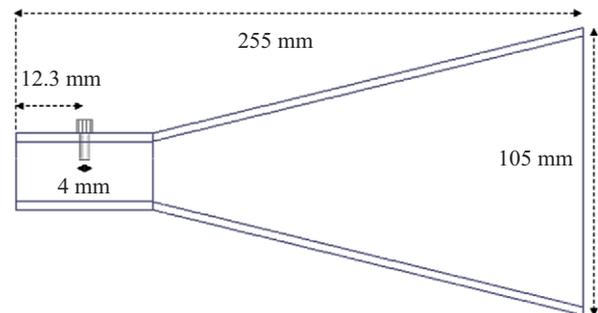

Fig. 3. Pyramidal horn antenna dimensions (side view).

and exhibited symmetrical patterns in the E-plane or H-plane; and (5) when the electromagnetic fields gradually propagate along the horn, the electric and magnetic fields pattern change from the waveguide pattern to that of the radiation pattern in free space, forming a uniform phase front with high directivity at the aperture.
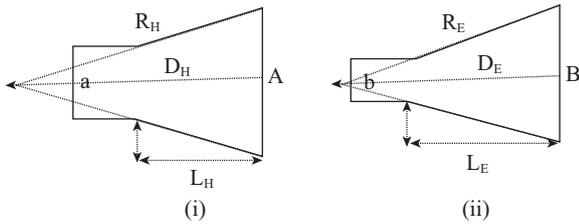
II. DESIGN CONSIDERATIONS

A typical horn antenna design comprises three parts: (1) the feed port on the horn; (2) the waveguide mode transformer (for rectangular waveguides, the dominant mode is TE_{10}; for conical waveguides, the dominant mode is TE_{11}); and (3) the radiating aperture on the horn. Horn antennas are typically excited using a connector probe or a waveguide port. The proposed pyramidal horn antenna uses a 3.5 mm SMA connector as the feed port. The excited wave front propagates along a WR187 rectangular waveguide and radiating outward via the pyramidal radiating aperture. A coaxial cable feed was connected to the waveguide, and HFSS software was used to simulate the optimal horn antenna dimensions before a prototype was fabricated. The side view of the horn antenna is depicted in Fig. 3 which shows the location of the feed port and the outer dimensions of the antenna.

A pyramidal horn antenna is constructed by extending the E-plane and H-plane of a rectangular waveguide (Braun, 1953; Braun, 1956), and its radiation characteristics are essentially a combination of the characteristics of the E-plane and H-plane

Table 1. Comparison of bit error rates for the simulation.

Parameter	mm	Parameter	mm
A	140.0	B	100.0
a	47.55	b	22.15
R_H	311.2	R_E	262.0
D_H	303.2	D_E	257.2
L_H	200.0	L_E	200.0

(i)   (ii)

Fig. 4. (i) H-plane (ii) E-plane of the pyramidal horn antenna.

Fig. 5. Photograph of the Prototype pyramidal horn antenna.

Fig. 6. Block diagram of a typical antenna measurement system.

of the horn antennas. The E- and H-planes are illustrated in Fig. 4 which shows the two cross-sectional views of the antenna. To construct an antenna that yields maximum gain, the aperture dimensions must simultaneously satisfy Eq. (1) and Eq. (2) (Guney and Hancer, 2003; Mayhew-Ridgers et al., 2000; Yaghjian, 1984) which are given as:

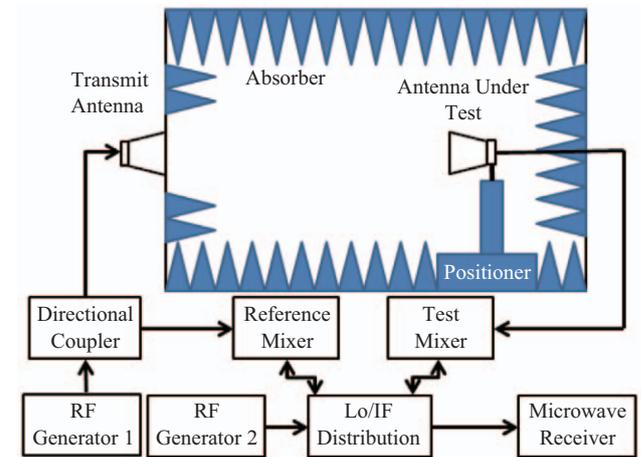$$A = \sqrt{3\lambda D_H} \qquad (1)$$

$$B = \sqrt{2\lambda D_E} \qquad (2)$$

The optimal gain (G) of the horn antenna can then be evaluated as:

$$G = \frac{4\pi\varepsilon AB}{\lambda^2} \qquad (3)$$

where, ε is the aperture efficiency, λ is the wavelength of the center frequency. The parameters A and B are as defined earlier, represent the dimensions of the horn aperture along the H-plane and E-plane, respectively. In Fig. 4, R_H and R_E give the diagonal lengths of the horn aperture in the H-plane and the E-plane, D_H and D_E represent the radii of the horn aperture in the H-plane and the E-plane; and L_H and L_E represent the distances between the two aperture planes and the WR187 rectangular waveguide, respectively. The optimized antenna dimensions are listed in Table 1. The simulated gain of ~17.3 dB at the center frequency gives an efficiency of ~0.82 by comparing to the theoretical ideal gain of ~18.2 dB evaluated using Eq. (3) with $\varepsilon = 1$. The simulated gain is comparable to the commercially available ETS-3160-05 horn antenna manufactured by ETS-Lindgren which gives a gain of ~17.1 dB. In general, the actual gain should be lower than the simulated one due to Ohmic loss and machining tolerance.

III. SIMULATION RESULTS AND EMPIRICAL ANALYSIS

Simulation, analysis, and modification of the design parameters were performed using commercial HFSS software (Ansoft Software). The photograph of the constructed pyramidal horn antenna is depicted in Fig. 5. The outer dimensions of the antenna are 145 mm (width) × 105 mm (height) × 255 mm (length). Data were measured using an antenna pattern measurement system (FR959) in the 500 MHz-40 GHz band in an anechoic chamber. A schematic block diagram of the anechoic chamber is depicted as Fig. 6. Detail description of the measurement setup of the anechoic chamber can be found elsewhere (Currie et al., 1970) and will not be mentioned here. In general, the setup is first calibrated by a standard gain horn and subsequently the test horn is in place to be measured. The received signal is frequency down shifted to IF range to be analyzed by a network analyzer. The separation between the transmit antenna and the test antenna in this setup is ~7 m which is much larger than the far field radiation range of the test antenna.
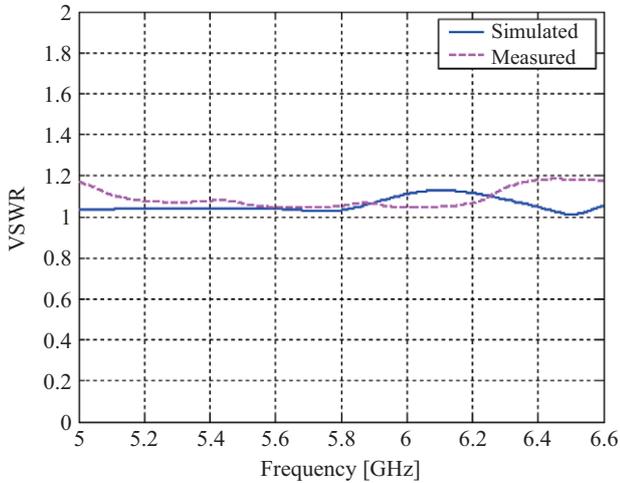
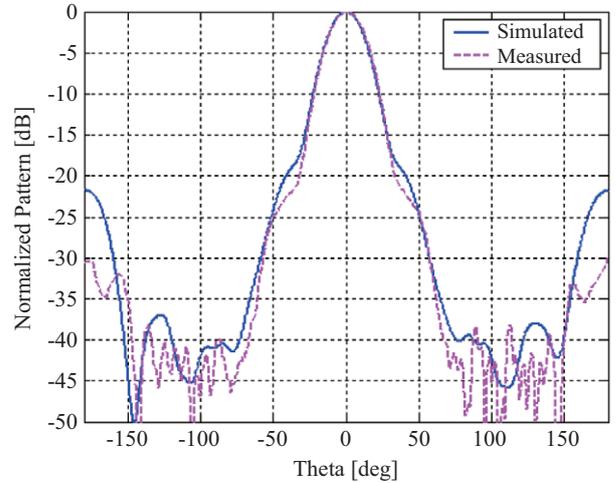**Fig. 7. Voltage standing wave ratio of the pyramidal horn antenna.**

Fig. 9. H-plane radiation pattern of the pyramidal horn antenna.
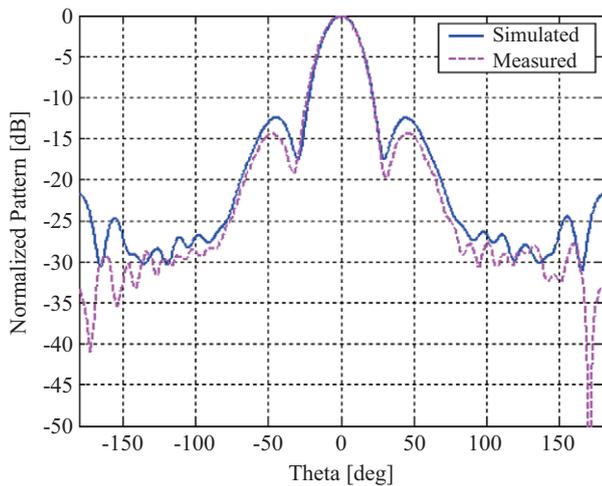

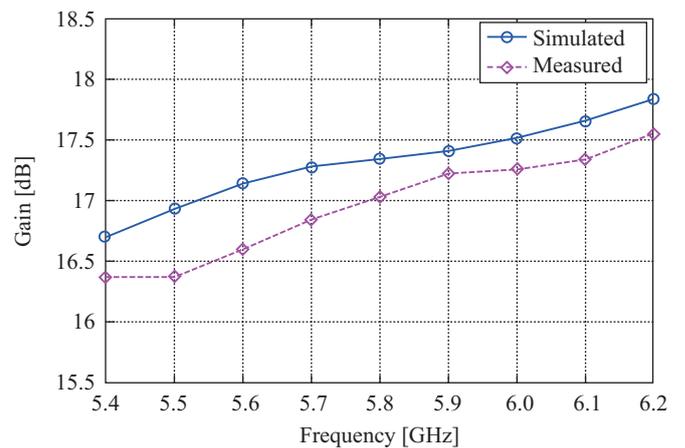**Fig. 8. E-plane radiation pattern of the pyramidal horn antenna.**

Fig. 10. Gain characteristics of the pyramidal horn antenna.

Fig. 7 shows a plot of the voltage standing wave ratio (VSWR) on the vertical axis versus the frequency on the horizontal axis (5 GHz-6.6 GHz). The solid line in the figure represents the simulated values according to the HFSS software analysis, and the dotted line represents the actual values obtained using the network analyzer. The results show that the VSWR values in the operating frequency range from 5.4 GHz-6.2 GHz are less than 1.2 for both the simulated and actual results, verifying that the electrical properties of the pyramidal horn antenna yielded excellent impedance matching, and conformed to the design requirements. Figs. 8 and 9 show the radiation patterns of the pyramidal horn antenna at the center frequency of 5.8 GHz in the E- and H-planes. The E-plane (Y-Z plane) and H-plane (X-Z plane) radiation patterns were plotted based on the normalized pattern on the vertical axis versus rotating angle θ with −180° ≤ θ ≤ 180° on the horizontal axis. The solid lines in the figures represent the simulated values according to HFSS software analysis and the

dotted lines represent the actual far-field measurements performed in an anechoic chamber. Within the frequency band, the E-plane and H-plane patterns are symmetrical. The measured E-plane and H-plane half power beam widths are approximately 26° and 25°, respectively. The experimental half power beam widths for both the E-plane and H-plane agreed well with that of the simulated values. The measured radiation pattern gains are larger than 16 dB in the frequency band. A detail illustration of the gain characteristics of the pyramidal horn antenna in the operating frequencies of 5.4-6.2 GHz is depicted in Fig. 10. The measured data show that the antenna exhibits close to flat gain characteristics throughout the frequency band with a gain ranged between 16 and 18 dB. In order for the designed horn antenna to be applicable in a WLRS set up, good directivity must be attained. This rather important feature is illustrated in Fig. 11 on the simulated 3D radiation pattern of the pyramidal horn antenna showing excellent directivity along both the E-plane and H-plane.
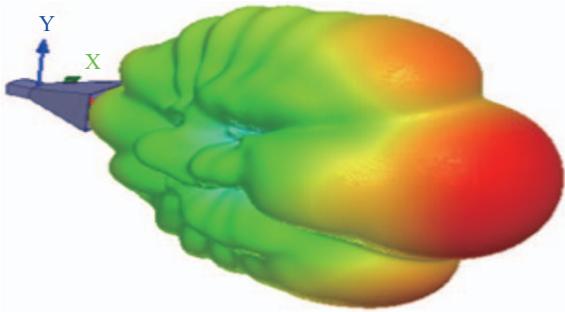
Fig. 11. 3D plot of the radiation pattern of the pyramidal horn antenna.

IV. CONCLUSIONS

This article presented the design, analysis, and simulation of a WLRS, using a pyramidal horn antenna that operates in the C-band. The High Frequency Structure Simulator software enables a quantitative evaluation of the optimum designs for signal frequency and broadband operation. The study showed that the prototype pyramidal horn antenna is capable of producing symmetric radiation patterns both in the E- and H-planes. The operating frequency range is from 5.4 GHz to 6.2 GHz with the central frequency at 5.8 GHz (a bandwidth of ~14%). The VSWR in the frequency range was measured to be smaller than 1.2 with near flat gain larger than 16 dB. The experimental measurements agreed well with the simulated results and conformed to the design specifications for the fabricated unit to operate as a key component of WLRS.

A WLRS comprises an antenna, radio frequency processing circuit, and solver module. The aim of this work is on the design of the antenna unit. Future works should consider the radio frequency processing circuits and solver modules used in the radar water-level sensors so that the implementation of domestic early warning for disaster prevention detection system can be realized.

REFERENCES

Ansoft Software Inc.. Ansoft simulator, version 12.0.

Balanis, C. A. (2005). Antenna Theory: Analysis and Design. John Wiley & Sons, New York, 769-783.

Braun, E. H. (1953). Gain of electromagnetic horns. Proc. IRE 41, 109-115.

Braun, E. H. (1956). Some data for the design of electromagnetic horns. IEEE Transactions on Antennas and Propagation 4, 29-31.

Currie, C. H., C. C. Morris and R. E. Pidgeon (1970). Microwave Antenna Measurements. Scientific-Atlanta, Inc. Georgia, chap.15.

Elliott, R. S. (2003). Antenna Theory and Design. John Wiley & Sons, New York.

Guney, K. and H. Hancer (2003). Improved formulas for narrow and wide aperture dimensions of optimum gain pyramidal horn. International Journal of RF and Microwave Computer-aided Engineering 13(3), 239-245.

Jasik, H. and R. C. Johnson (2000). Antenna Engineering Handbook. McGraw-Hill, New York.

Mayhew-Ridgers, G., J. W. Odendaal and J. Joubert (2000). On primary incident wave models for pyramidal horn gain calculations. IEEE Transactions on Antennas and Propagation 48(8), 1246-1252.

Yaghjian, A. D. (1984). Approximate formulas for the far field and gain of open-ended rectangular waveguides. IEEE Transactions on Antennas and Propagation 32(4), 378-384.